

A decline in atmospheric CO₂ levels under negative emissions may enhance carbon retention in the terrestrial biosphere

So-Won Park ¹ & Jong-Seong Kug ^{1,2} 

Negative emissions are a key mitigation measure in emission scenarios consistent with Paris agreement targets. The terrestrial biosphere is a carbon sink that regulates atmospheric carbon dioxide (CO₂) concentration and climate, but its role under negative emissions is highly uncertain. Here, we investigate the reversibility of the terrestrial carbon cycle to idealized CO₂ ramp-up and ramp-down forcing using an ensemble of CMIP6 Earth system models. We find a strong lag in the response of the terrestrial carbon cycle to CO₂ forcing. The terrestrial biosphere retains more carbon after CO₂ removal starts, even at equivalent CO₂ levels. This lagged response is greatest at high latitudes due to long carbon residence time and enhanced vegetation productivity. However, in the pan-Arctic region, terrestrial carbon dynamics under negative emissions are highly dependent on permafrost processes. We suggest that irreversible carbon emissions may occur in permafrost even after achieving net-zero emissions, which offsets ~30% of enhanced land C retention and could hinder climate mitigation.

¹Division of Environmental Science and Engineering, Pohang University of Science and Technology (POSTECH), Pohang, South Korea. ²Institute for Convergence Research and Education in Advanced Technology, Yonsei University, Seoul, South Korea. ✉email: jskug@postech.ac.kr

Cumulative emissions of anthropogenic carbon dioxide (CO₂) have been driving long-term global warming^{1–3}, which has negatively impacted the physical environment, ecosystem, and humanity^{4,5}. To minimize the potential risks of climate change, the 2015 Paris Agreement aims to keep global warming well below 2 °C above pre-industrial levels and pursue efforts to limit it to 1.5 °C above pre-industrial levels⁶. Modeled pathways to limit global warming to 1.5 °C indicate emissions need to reach net zero, and net-negative emissions (i.e. a decline in atmospheric CO₂ levels) are required to return global warming to 1.5 °C following a temperature overshoot⁷. To accomplish this, anthropogenic emissions must be reduced and carbon dioxide removal (CDR), which permanently removes CO₂ from the atmosphere, is likely required^{7–10}.

Despite the increasing attention on CDR in political and economic discussions, there remain uncertainties in the effectiveness of CDR due to a poor understanding of the future behavior of the Earth system to reduced atmospheric CO₂ levels^{11–14}. The terrestrial biosphere is a natural carbon (C) sink that removes a large fraction of anthropogenic CO₂ from the atmosphere¹⁵. However, there are uncertainties in the future behavior of the terrestrial carbon cycle^{16–18}, especially their response under net-negative emissions; thus, there is an urgent need for a better understanding of terrestrial C fluxes after reaching net-zero.

To date, studies on the reversibility of land C pool have been conducted based on idealized CO₂ ramp-up and ramp-down forcing experiments using Earth system models (ESMs)^{19–21}. Despite similar experimental designs, studies have shown considerable differences in the response of land C stocks to CO₂ forcing: the temporal evolution, the extent of change, and its spatial characteristics^{19–21}. For example, a previous study²¹ reported that land C stores are largely reversible within the timescale of changing CO₂ due to the balance between an overshoot in the tropics and delayed response in the northern high latitudes. On the other hand, other studies^{19,20} reported that the terrestrial biosphere continues to remove CO₂ immediately after the start of CO₂ ramp-down due to inertia in vegetation dynamics and soil C pool, and as a result, stores more C at the end of the simulation than in its initial state.

Inconsistencies in the literature lead to uncertainties in estimates of land C fluxes after net-zero emissions are reached. This hinders establishing effective climate mitigation strategies and thus highlights the need for a multimodel approach and a better understanding of the terrestrial C cycle response to negative emission and its underlying mechanisms. Here, we analyze eight ESMs from the Coupled Model Intercomparison Project Phase 6 (CMIP6)²², which performed the climate and carbon cycle reversibility experiment¹² (see “Methods” and Supplementary Tables 1, 2), to assess the reversibility of terrestrial C flux and stock in a multimodel context. In this experiment, atmospheric CO₂ concentrations are prescribed to increase at 1% year until quadrupling (~139 years) and then decrease at the same rate until reaching pre-industrial CO₂ levels, after which the simulation continues for at least 60 years.

Results

Lagged response of global terrestrial carbon fluxes and stocks.

First, the multimodel mean (MME) temporal evolutions of key variables corresponding to the ramp-up and ramp-down CO₂ forcing were examined (Fig. 1). The global mean land surface air temperature (SAT) anomaly increased by ~6.7 K and peaked at model Year 144, after which it decreased with a slower rate of change than observed during the ramp-up period. Land temperatures show a delayed response due to the thermal inertia of the ocean^{23,24} and remain ~1 K higher than the initial state until the end of the simulation. Land precipitation (PRCP) follows land

temperature^{25,26}, showing a peak with a 4-year delay after that of temperature and a greater response on the ramp-down CO₂ pathway. However, the land PRCP anomaly exhibited large internal variability and a wide range of inter-model spread.

The changes in climate system and atmospheric CO₂ concentration affected terrestrial C fluxes by regulating terrestrial ecosystem processes. At a global scale, net primary production (NPP), synonymous with net carbon uptake by vegetation, linearly increased and subsequently decreased, showing an almost reversible response that was mainly attributable to the CO₂ fertilization effect^{27–29}. However, heterotrophic respiration (Rh) exhibited a lagged response to CO₂ forcing and slowly decreased during the ramp-down period. This is mainly because Rh changes in proportion to the C pool altered by changes in NPP, but there is a time lag between changes in NPP, C sequestration, and its release through microbial respiration^{30–33}. The delayed increase of litter-soil C content increased the decomposition during the CO₂ ramp-down period despite the same CO₂ level³³. In addition, warmer and wetter conditions on CO₂ ramp-down pathway likely enhanced microbial activity^{34–36}, thereby partly contributing to the lagged response of Rh.

The net atmosphere-to-land C flux, net biome productivity (NBP), mainly determined by the imbalance between NPP and Rh, also exhibited a lagged response. NBP was positive during the CO₂ ramp-up period, demonstrating a well-known role of the land as a C sink¹⁵. NBP rapidly increased during the initial period, but it soon became relatively constant due to the declining effect of CO₂ fertilization^{37,38}. The terrestrial biosphere continues to uptake ~43 Gt C for decades after the CO₂ concentration begins to decrease. Although the CO₂ is prescribed in the present modeling experiments, this result suggests that the terrestrial ecosystem will further contribute to the reduction of CO₂ concentration for decades after achieving net-zero emissions, thereby lessening the reliance on CDR, in line with the previous literature^{19,20,39,40}.

Thereafter, the terrestrial biosphere becomes a C source as Rh exceeds NPP due to the lagged response of Rh. During the remainder of CO₂ ramp-down period, NBP gradually decreased, showing a maximum negative value at the end of the ramp-down period. This result implies that climate mitigation policy should be designed taking into account terrestrial ecosystem C that will be released under negative emissions. During the restoring period, NBP showed a tendency to return to its initial state. Overall, these responses in NBP led to a lag in the total land C stock. The total land C stock anomaly continued to increase immediately after CO₂ ramp-down began, with the land retaining more C than its pre-industrial level until the end of the simulation, indicating its positive role in mitigating anthropogenic climate change.

Latitudinal dependency of the lagged response of the terrestrial carbon cycle.

Latitudinal differences in the response of the physical climate system and terrestrial C cycle to CO₂ forcing were identified (Fig. 2). Land temperature showed a similar timescale of the delayed response to CO₂ forcing at all latitudes, and remained warmer than its initial state for the entire simulation period. Precipitation in the northern mid-high latitudes showed a similar evolution to the global mean, but with a heterogeneous response between 60°S–20°N. In the northern mid-high latitudes where cold temperature limits vegetation growth^{41,42}, the lagged response of the climate system resulted in warmer and wetter conditions during CO₂ ramp-down period, which enhanced photosynthesis and lengthened the growing season. However, in the tropics where the temperatures are close to the optimal temperature for photosynthesis⁴³ and precipitation decreased during the CO₂ ramp-down period (Supplementary Fig. 1), the

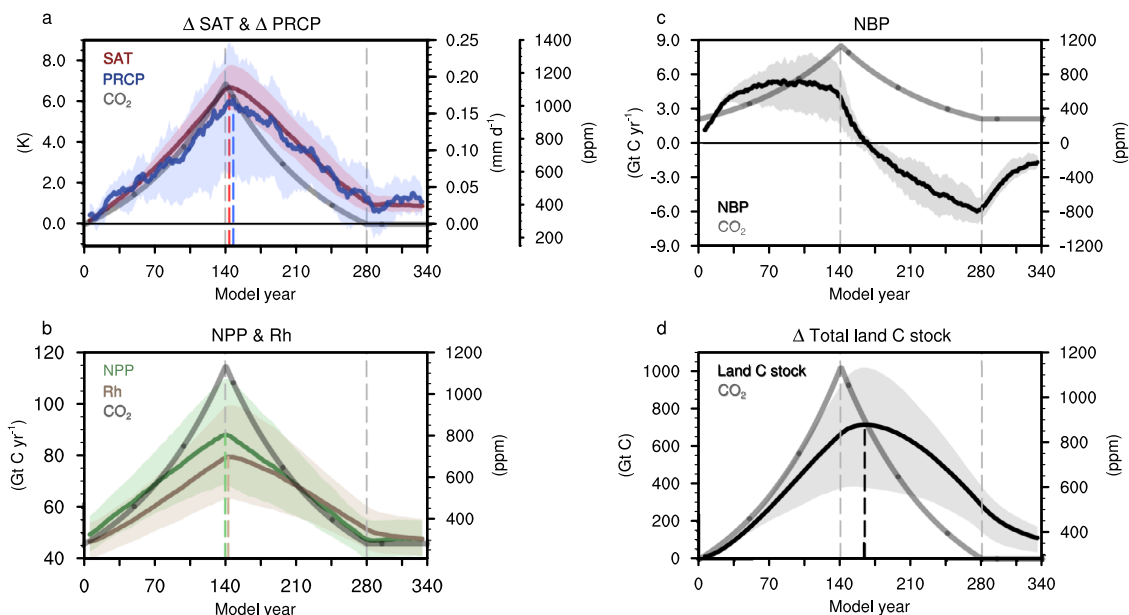


Fig. 1 Temporal evolution of global terrestrial carbon fluxes and stock. **a–d** Time-series of annual mean land surface air temperature (SAT) and precipitation (PRCP) anomaly (**a**), annual net primary production (NPP) and heterotrophic respiration (Rh) (**b**), annual net biome productivity (NBP) (**c**), and annual mean total land C stock anomaly (**d**). All values are calculated over the global land area excluding Antarctica. The solid lines and shadings show the MME mean and the range of 95% confidence level based on the bootstrap method. All calculations were conducted after taking the 11-year running mean. The beginning and end of CO₂ changes are indicated by the gray dashed vertical line.

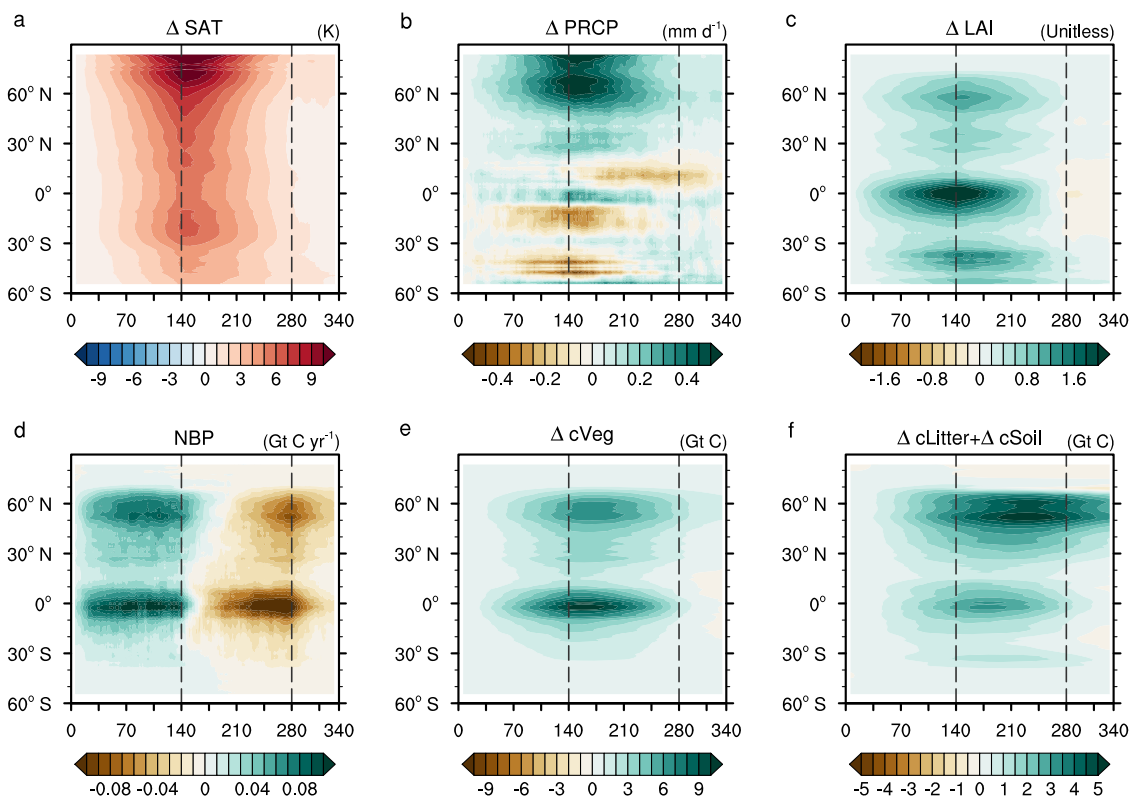


Fig. 2 Latitudinal differences in the response of the climate system and terrestrial carbon cycle to CO₂ forcing. **a–f** Time-latitude diagrams of annual mean anomalies of changes in land SAT (**a**), land PRCP (**b**), and leaf area index (LAI) (**c**). The zonal sum of annual NBP (**d**), vegetation carbon (cVeg) anomaly (**e**) and sum of cLitter and cSoil anomalies (**f**). All values are MME and smoothed by the 11-year moving average. The beginning and end of CO₂ changes are indicated by the gray dashed vertical line.

leaf area index (LAI), an indicator of vegetation growth, rapidly decreased after the CO₂ peak. Therefore, LAI in the tropics showed a reversible response within the timescale of CO₂ change, but with the LAI response to CO₂ forcing becoming increasingly delayed at higher latitudes.

The latitudinal dependence of the terrestrial biosphere response was more evident in the evolution of NBP. The terrestrial biosphere in the mid-high latitudes continued to absorb C for decades after atmospheric CO₂ concentrations decreased. This was due to the formation of favorable climate conditions for vegetation growth, and thus the transition of C sinks to sources was more delayed than in the tropics. Accordingly, the annual mean vegetation carbon (cVeg) anomaly was almost reversible in the tropics, whereas the mid-high latitudes retain more C after the CO₂ peak due to the longer timescale of reversibility.

The annual mean C anomaly stored in the litter–soil system also exhibited latitudinally dependent delayed response similar to cVeg, but with a greater time lag to CO₂ forcing because of the C flow from plant biomass to soil–litter decay. The increase of litter–soil C and its delay were greatest in high latitude regions with longer C residence (or turnover) time due to slow decomposition in cold environments^{44–46}. Consequently, because of this latitudinal dependency, the lagged response of global land C stock is mostly attributable to the mid-high latitudes, not the tropics, constituting most of the global land C stock anomaly after the end of CO₂ forcing (Supplementary Table 3 and Supplementary Fig. 1).

Inter-model diversity of terrestrial carbon cycle response to CO₂ forcing and its regional characteristics. There was considerable inter-model diversity in the lagged responses of the terrestrial C cycle to CO₂ forcing (Supplementary Fig. 2). The extent of the difference in global land C stock between the ramp-down and ramp-up period was dependent on how much C was stored during CO₂ ramp-up period, which was related to NPP sensitivities to increased CO₂ (dNPP/dCO₂) (Supplementary Fig. 3). This NPP sensitivity to CO₂ can be expressed as the product of carbon use efficiency (CUE: dNPP/dGPP, the fraction of GPP turned into NPP after considering autotrophic respiration losses) and strength of CO₂ fertilization (dGPP/dCO₂). The higher CUE and stronger CO₂ fertilization effect lead to the greater increase in land C storage. For example, ACCESS-ESM1-5 exhibited the lowest dNPP/dCO₂ due to its weak CO₂ fertilization effect and the low CUE⁴⁷ and hence almost reversible response of the terrestrial C stock.

The MME pattern of the land C pool anomaly differs from previous single model results^{19,21}: the amplitude and spatial pattern of land C stock changes differ between ESMs (Supplementary Figs. 4 and 5). Moreover, the peak of land C stock and the timescale of lagged response to CO₂ forcing are diverse. These results imply that a single model study cannot draw a concrete conclusion due to large uncertainties. Exploring inter-model diversity can advance our understanding of the future terrestrial carbon cycle in the ESMs and nature. Differences in representations of terrestrial processes and climate change between ESMs may be responsible for this large inter-model diversity. In the tropics and high latitudes, the inter-model spread is considerable, but it cannot be fully explained by the sensitivity of vegetation productivity to increased CO₂ (Supplementary Fig. 3). Though previous studies pointed to the importance of nitrogen cycling and dynamic vegetation^{19,39,47,48}, there is no significant impact of the inclusion of these processes on inter-model spread⁴⁰.

Therefore, to further understand the regional responses and their inter-model diversity, we investigated the spatial pattern of the lagged response of total land C stock (Fig. 3a, b). The total land C stock during the CO₂ ramp-down phase was distinctly higher than that during the CO₂ ramp-up phase despite the same CO₂ concentration, especially in boreal forests, Maritime

Continents, and East Asia. In particular, boreal forests can store C for a long time owing to the long turnover time of soil C^{44–46,49}. However, the differences in the land C stock in Amazon (details in Supplementary Note 1) and permafrost regions are statistically insignificant due to the diverse response among ESMs (Supplementary Figs. 6 and 7). Inter-model diversity, as estimated by the coefficient of variation, is highest in the continents above 60°N (Fig. 3c, d), indicating the greatest relative variability in high latitudes. This is because of two exceptional models (CESM2 and NorESM2-LM), which simulate lower land C stock in the ramp-down period than in the ramp-up period, especially in permafrost regions (Supplementary Figs. 5, 6 and 8).

Irreversible carbon release to the atmosphere in permafrost region. We conducted a more detailed analysis to understand the contrasting terrestrial C stock response to CO₂ forcing in permafrost regions (Fig. 4). Most models showed a positive cSoil anomaly due to the lagged response at the end of changing CO₂, but CESM2 and NorESM2-LM exhibited a negative cSoil anomaly. This is attributed to a faster transition of land C sinks to sources (~80 years faster than the other models) without a lagged response due to the sharp increase of Rh. Notably, only these two ESMs, coupled with Community Land Model 5, include the representation of deep and frozen soil C and hence permafrost C pools (Supplementary Note 2)^{50,51}. Vertically resolved soil biogeochemistry enables the model to generate large C stocks in the permafrost domain, as observed (1460–1600 Pg C)^{50,52,53}. Consequently, these two models (~1466 Gt C) simulate ~7 times greater cSoil climatology than the other ESMs (~206 Gt C). Therefore, they include the C decomposition in the permafrost zone containing large soil organic C and thus simulate a negative cSoil anomaly. However, the soil C stock in the other models is remarkably low compared to the observed value due to the absence of permafrost and related processes, so they possibly underestimate the soil respiration (Supplementary Fig. 9).

As a result, CESM2 and NorESM2-LM (group A) simulated C release to the atmosphere in the permafrost region from the later parts of the ramp-up period due to enhanced microbial C decomposition under warmer conditions. This indicates that permafrost regions could be a net C source rather than a C sink over the course of the CO₂ ramp-up and ramp-down forcing, implying its accelerating role in global warming. However, the other models (group B) showed a transition from C sink to source that is similar to the global mean response of NBP but much slower due to the greater lag at high latitudes.

Consequently, group B models simulated a positive total land C stock anomaly over the entire experimental period due to their lagged response to CO₂ forcing. In group B models, the terrestrial biosphere serves as a C sink, storing more C (~38 Gt C) at the end of the simulation than in its initial state. However, the land C stock anomaly in group A models, including the permafrost C pool, showed quite different behavior with the total land C stock slightly increasing in the early phase of the ramp-up period but gradually declining thereafter. As a result, the permafrost lost ~33 Gt C by the end of the restoring period compared to the pre-industrial period, offsetting ~30% of enhanced land C retention due to the lagged response of the terrestrial C cycle (Supplementary Table 3). This suggests that an evident irreversible response to CO₂ forcing could worsen global warming.

Discussion

In this study, we investigated the reversibility of land C fluxes and stocks to CO₂ forcing in idealized CO₂ ramp-up and ramp-down simulations and especially focused on their responses under

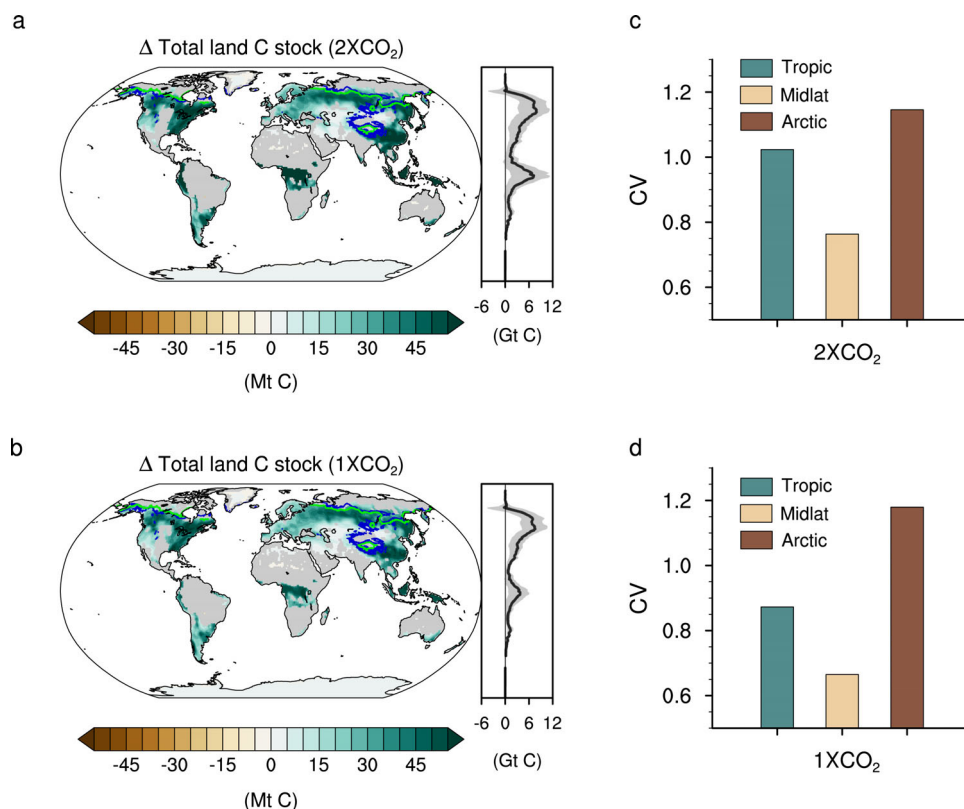


Fig. 3 Lagged response of terrestrial carbon cycle and its inter-model spread. **a, b** Difference of MME anomalies of total land C stock between model Year 210 and 70 ($2 \times \text{CO}_2$) (**a**). MME anomalies of total land C stock at model Year 280 ($1 \times \text{CO}_2$) (**b**). The zonal sum is plotted on the right side of the map. Only significant values at the 95% confidence level, based on the bootstrap method, are shown. The simulated MME permafrost extent and boundaries of continuous and discontinuous permafrost from the CCI-PF data (see “Methods”) are superimposed in green and blue, respectively. **c, d** Coefficients of variation (CV: the standard deviation of the spread divided by the mean) of the difference in the total land C stock between model Year 210 and 70 ($2 \times \text{CO}_2$) (**c**) and total land C stock anomalies at model Year 280 ($1 \times \text{CO}_2$) (**d**) in the tropics (30°S – 30°N), mid-latitudes (30° – 60°N), and high-latitudes (above 60°N). All calculations were conducted after taking the 11-year running mean.

negative emissions. Total land C stocks exhibit a lagged response to CO_2 forcing; even after CO_2 removal starts, land C maintains considerably higher levels compared to that in the ramp-up period at the same CO_2 level. This lagged response of the terrestrial C cycle is latitudinally dependent, and the timescale of reversibility is much longer in high-latitude regions. At a regional scale, boreal forests, East Asia, and Maritime Continents can store C for longer than other regions under net-negative emissions. These spatiotemporal characteristics can be considered for establishing an effective strategy for natural climate solutions, such as forest management.

To deal with the inconsistency among the results of the previous studies, we examined the multi-model response using eight ESMs from CMIP6. The lag in global terrestrial C stock response is mostly attributable to the mid-high latitudes because the inertia of soil C pool is greatest at high latitudes. In addition, the lag in the climate system response in the mid-high latitudes also contributes to this by enhancing vegetation productivity during the ramp-down period. Through the inter-model comparison, we found that the intermodel diversity in the lagged response of the terrestrial C stock is considerable and largely explained by the different NPP sensitivity to increased CO_2 between ESMs. We also pointed out that the diverse precipitation response in the Amazon to CO_2 forcing and the inclusion of permafrost C pools are important factors in increasing the inter-model spread of response of the land C stock to CO_2 forcing.

We have demonstrated that irreversible permafrost C loss would considerably hinder efforts to mitigate global warming

even if we achieve net-zero emissions. This should be considered in climate policy discussions and decisions. In particular, we quantitatively examined the role of permafrost in asymmetric terrestrial C cycle response to CO_2 forcing, thereby advancing our understanding of previously identified knowledge gap^{19,39,40}. However, more careful quantification is further needed as no land surface model considers abrupt thawing: the rapid degradation of ice-rich permafrost^{54,55}. Our findings include uncertainties resulting from model biases associated with permafrost processes and their initialization procedures (Supplementary Note 2), which should be taken into account and further examined.

We note that the present experimental design (up to $4 \times \text{CO}_2$) results in larger changes in land SAT and C stock compared to those changes under the SSP5-3.4-overshoot scenario⁴⁰, which may lead to an excessive nonlinear response. Understanding the nonlinear and variable responses of the terrestrial C cycle according to the rate of CO_2 change or under the different CO_2 pathways is further needed for effective climate policy.

Methods

CMIP6-CDRMIP data and experimental design. The climate and carbon cycle reversibility experiment (short name: CDR-reversibility) from the CMIP6 Carbon Dioxide Removal Model Intercomparison Project (CDRMIP)¹² was analyzed to investigate the carbon cycle response to large-scale CO_2 removal. This experiment was branched from the *1pctCO2* experiment, in which the CO_2 level increases at a rate of $1\% \text{ yr}^{-1}$ from pre-industrial levels to quadrupling for 140 years, from the CMIP6 Diagnostic, Evaluation, and Characterization of Klima (DECK)²². The *piControl* experiment, which started after the model spin-up during which the climate begins to come into balance with

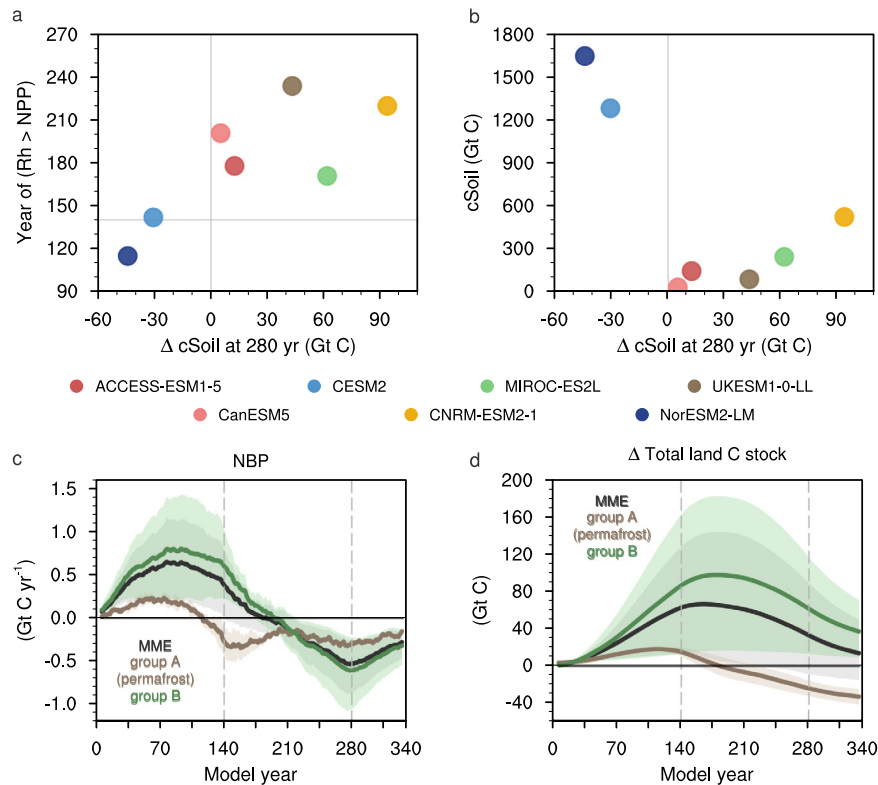


Fig. 4 Irreversible terrestrial carbon loss in the permafrost region. a, b Scatterplot of the cSoil anomalies at model Year 280 versus the model year when Rh exceeds NPP (**a**). Scatterplot of the cSoil anomalies at model Year 280 versus the mean state of cSoil in the control simulation (**b**). **c, d** Time-series of annual NBP (**c**) and total land C stock anomalies (**d**): the MME mean (black), the average value from ESMs, including permafrost representation (brown, group A), and the average value for the other models (green, group B). The shadings represent the 95% confidence intervals based on the bootstrap method. The beginning and end of CO₂ changes are indicated by the gray dashed vertical line. All values are averaged over the permafrost region above 60°N and smoothed by the 11-year moving average.

forcing, serves as a baseline for *1pctCO2* experiment. Then, a 1% yr⁻¹ removal of CO₂ from the atmosphere is prescribed for 140 years until the pre-industrial CO₂ level is reached and then held for as long as possible (minimum of 60 years) in the *1pctCO2-cdr* simulation (minimum of 200 years). Thus, the total length of the CDR-reversibility experiment employed herein is 340 years. We calculated the anomalies of CDR-reversibility simulations using the pre-industrial control simulation (*piControl*) from DECK as a baseline.

We used eight ESMs (ACCESS-ESM1-5, CanESM5, CESM2, CNRM-ESM2-1, GFDL-ESM4, MIROC-ES2L, NorESM2-LM, and UKESM1-0-LL), which were coupled with the full carbon cycle and performed the CDR-reversibility experiment (Supplementary Tables 1, 2). The MME mean was derived by regridding the outputs from ESMs to a common 1° × 1° grid, then averaging them. GFDL-ESM4 does not provide cLitter and cSoil data, UKESM1-0-LL does not provide cLitter data, and NorESM2-LM does not provide precipitation data. Due to this limitation, GFDL-ESM4 and UKESM1-0-LL were excluded when calculating the MME mean of total land C stock. Herein, the bootstrap method was used to test the statistical significance of the difference between the experiments. For MME, eight values were randomly selected from eight ESMs with replacements, and then, their average was computed. By repeating this process 1000 times, the confidence intervals were determined, and only significant values were shown to indicate the model agreement.

Diagnosing the permafrost extent in the model. The permafrost extent in the model was diagnosed using the temperature at the minimum soil depth (D_{zsa}) where the monthly mean variation of soil temperature within a year is <0.1 °C⁵⁶. If the temperature at D_{zsa} is <0 °C for 2 years or more, that grid cell is assumed to be permafrost. However, there are most CMIP6 models in which a soil profile is not deep enough to identify D_{zsa} (Supplementary Table 2). For such models, permafrost is assumed to be present in grid cells where the 2-year mean soil temperature of the deepest soil layer is <0 °C⁵⁷. The extent of permafrost in the model was diagnosed using *piControl* simulation, except for GFDL-ESM4M, which does not provide soil layer temperature data. In the multimodel context, if the grid cell is diagnosed as permafrost in four or more of the seven ESMs, we define those grid cells as permafrost regions. The MME permafrost extent is almost similar to the

boundaries of permafrost extent (>50% coverage) from ESA Climate Change Initiative permafrost (CCI-PF) reanalysis dataset⁵⁸ (Fig. 3a, b).

Data availability

All data used in this study are publicly available and can be downloaded from the corresponding websites (CMIP6: <https://esgf-node.lnl.gov/projects/cmip6/>; ESA CCI-PF: <https://apc.awi.de/dataset/pepx>).

Code availability

The computer codes that support the analysis within this paper are available from the corresponding author on request.

Received: 24 August 2022; Accepted: 9 November 2022;

Published online: 19 November 2022

References

- Allen, M. R. et al. Warming caused by cumulative carbon emissions towards the trillionth tonne. *Nature* **458**, 1163–1166 (2009).
- Matthews, H. D., Gillett, N. P., Stott, P. A. & Zickfeld, K. The proportionality of global warming to cumulative carbon emissions. *Nature* **459**, 829–832 (2009).
- Collins, M. R. et al. Long-term Climate Change: Projections, Commitments and Irreversibility. In *Climate Change 2013: The Physical Science Basis* (eds Stocker, T. F. et al.) 1029–1136 (IPCC, Cambridge Univ. Press, 2013).
- IPCC *Climate Change 2014: Impacts, Adaptation, and Vulnerability* (eds Field, C. B. et al.) (Cambridge Univ. Press, 2014).
- Carleton, T. A. & Hsiang, S. M. Social and economic impacts of climate. *Science* **353**, aad9837 (2016).

6. UNFCC. Adoption of the Paris Agreement *FCCC/CP/2015/L.9/Rev.1*, 1–32 (Paris, France: UNFCCC, 2015).
7. Rogelj, J. et al. In *Special Report on Global Warming of 1.5 °C* (eds Masson-Delmotte, V. et al.) 93–174 (IPCC, Cambridge Univ. Press, 2018).
8. Gasser, T., Guivarch, C., Tachiiri, K., Jones, C. D. & Ciais, P. Negative emissions physically needed to keep global warming below 2 °C. *Nat. Commun.* **6**, 7958 (2015).
9. Rogelj, J. et al. Differences between carbon budget estimates unravelled. *Nat. Clim. Chang.* **6**, 245–252 (2016).
10. Kriegler, E. et al. Pathways limiting warming to 1.5 °C: a tale of turning around in no time? *Philos. Trans. R. Soc. A Math. Phys. Eng. Sci.* **376**, 20160457 (2018).
11. Rogelj, J., Forster, P. M., Kriegler, E., Smith, C. J. & Séférian, R. Estimating and tracking the remaining carbon budget for stringent climate targets. *Nature* **571**, 335–342 (2019).
12. Keller, D. P. et al. The Carbon Dioxide Removal Model Intercomparison Project (CDRMIP): rationale and experimental protocol for CMIP6. *Geosci. Model Dev.* **11**, 1133–1160 (2018).
13. Rogelj, J. et al. Mitigation pathways compatible with 1.5 °C in the context of sustainable development. In *Global warming of 1.5 °C. An IPCC special report on the impacts of global warming of 1.5 °C above pre-industrial levels and related global greenhouse gas emission pathways, in the context of strengthening the global response to the threat of climate change, sustainable development, and efforts to eradicate poverty* (eds Masson-Delmotte, V. et al.) (2018) In Press.
14. Damon Matthews, H. et al. An integrated approach to quantifying uncertainties in the remaining carbon budget. *Commun. Earth Environ.* **2**, 1–11 (2021).
15. Friedlingstein, P. et al. Global Carbon Budget 2020. *Earth Syst. Sci. Data* **12**, 3269–3340 (2020).
16. Friedlingstein, P. et al. Climate–carbon cycle feedback analysis: results from the C4MIP model intercomparison. *J. Clim.* **19**, 3337–3353 (2006).
17. Heimann, M. & Reichstein, M. Terrestrial ecosystem carbon dynamics and climate feedbacks. *Nature* **451**, 289–292 (2008).
18. Keenan, T. F. & Williams, C. A. The terrestrial carbon sink. *Annu. Rev. Environ. Resour.* **43**, 219–243 (2018).
19. Boucher, O. et al. Reversibility in an Earth System model in response to CO₂ concentration changes. *Environ. Res. Lett.* **7**, 024013 (2012).
20. Zickfeld, K., MacDougall, A. H. & Damon Matthews, H. On the proportionality between global temperature change and cumulative CO₂ emissions during periods of net negative CO₂ emissions. *Environ. Res. Lett.* **11**, 055006 (2016).
21. Ziehn, T., Lenton, A. & Law, R. An assessment of land-based climate and carbon reversibility in the Australian Community Climate and Earth System Simulator. *Mitig. Adapt. Strateg. Glob. Chang.* **25**, 713–731 (2020).
22. Eyring, V. et al. Overview of the Coupled Model Intercomparison Project Phase 6 (CMIP6) experimental design and organization. *Geosci. Model Dev.* **9**, 1937–1958 (2016).
23. Wigley, T. M. L. The climate change commitment. *Science* **307**, 1766–1769 (2005).
24. Hare, B. & Meinshausen, M. How much warming are we committed to and how much can be avoided? *Clim. Change* **75**, 111–149 (2006).
25. Wu, P., Wood, R., Ridley, J. & Lowe, J. Temporary acceleration of the hydrological cycle in response to a CO₂ rampdown. *Geophys. Res. Lett.* **37**, L12705 (2010).
26. Cao, L., Bala, G. & Caldeira, K. Why is there a short-term increase in global precipitation in response to diminished CO₂ forcing? *Geophys. Res. Lett.* **38**, L06703 (2011).
27. Gunderson, C. A. & Wullschlegel, S. D. Photosynthetic acclimation in trees to rising atmospheric CO₂: A broader perspective. *Photosynth. Res.* **39**, 369–388 (1994).
28. Drake, B. G., González-Meler, M. A. & Long, S. P. More efficient plants: a consequence of rising atmospheric CO₂? *Annu. Rev. Plant Physiol. Plant Mol. Biol.* **48**, 609–639 (1997).
29. Ainsworth, E. A. & Long, S. P. What have we learned from 15 years of free-air CO₂ enrichment (FACE)? A meta-analytic review of the responses of photosynthesis, canopy properties and plant production to rising CO₂. *New Phytol.* **165**, 351–372 (2005).
30. Friedlingstein, P. et al. On the contribution of CO₂ fertilization to the missing biospheric sink. *Global Biogeochem. Cycles* **9**, 541–556 (1995).
31. Thompson, M. V., Randerson, J. T., Malmström, C. M. & Field, C. B. Change in net primary production and heterotrophic respiration: How much is necessary to sustain the terrestrial carbon sink? *Global Biogeochem. Cycles* **10**, 711–726 (1996).
32. Kicklighter, D. W. et al. A first-order analysis of the potential role of CO₂ fertilization to affect the global carbon budget: a comparison of four terrestrial biosphere models. *Tellus B Chem. Phys. Meteorol.* **51**, 343–366 (1999).
33. Chimuka, V. R., Nzotungicimpaye, C. & Zickfeld, K. Quantifying land carbon cycle feedbacks under negative CO₂ emissions. Preprint at *Biogeosci. Discuss.* <https://doi.org/10.5194/bg-2022-168> (2022).
34. Orchard, V. A. & Cook, F. J. Relationship between soil respiration and soil moisture. *Soil Biol. Biochem.* **15**, 447–453 (1983).
35. Schlesinger, W. H. & Andrews, J. A. Soil respiration and the global carbon cycle. *Biogeochemistry* **48**, 7–20 (2000).
36. Bond-Lamberty, B. & Thomson, A. Temperature-associated increases in the global soil respiration record. *Nature* **464**, 579–582 (2010).
37. Chapin F. S. III & Eviner V. T. In *Treatise on Geochemistry* 2nd edn. (eds Holland H. D. & Turekian K. K.) 189–216 (Elsevier, 2014).
38. Zickfeld, K., Azevedo, D., Mathesius, S. & Matthews, H. D. Asymmetry in the climate–carbon cycle to positive and negative CO₂ emissions. *Nat. Clim. Chang.* **11**, 613–617 (2021).
39. MacDougall, A. H. et al. Is there warming in the pipeline? a multi-model analysis of the zero emissions commitment from CO₂. *Biogeosciences* **17**, 2987–3016 (2020).
40. Koven, C. et al. 23rd Century surprises: Long-term dynamics of the climate and carbon cycle under both high and net negative emissions scenarios. *Earth Syst. Dyn. Discuss.* **1**–32 (2021).
41. Xu, L. et al. Temperature and vegetation seasonality diminishment over northern lands. *Nat. Clim. Chang.* **3**, 581–586 (2013).
42. Zhu, Z. et al. Greening of the Earth and its drivers. *Nat. Clim. Chang.* **6**, 791–795 (2016).
43. Doughty, C. E. & Goulden, M. L. Are tropical forests near a high temperature threshold? *J. Geophys. Res. Biogeosci.* **113**, G00B07 (2008).
44. Bird, M. I., Chivas, A. R. & Head, J. A latitudinal gradient in carbon turnover times in forest soils. *Nature* **381**, 143–146 (1996).
45. Bloom, A. A., Exbrayat, J. F., Van Der Velde, I. R., Feng, L. & Williams, M. The decadal state of the terrestrial carbon cycle: Global retrievals of terrestrial carbon allocation, pools, and residence times. *Proc. Natl. Acad. Sci. USA* **113**, 1285–1290 (2016).
46. Wang, J. et al. Soil and vegetation carbon turnover times from tropical to boreal forests. *Funct. Ecol.* **32**, 71–82 (2018).
47. Arora, V. K. et al. Carbon–concentration and carbon–climate feedbacks in CMIP6 models and their comparison to CMIP5 models. *Biogeosciences* **17**, 4173–4222 (2020).
48. Davies-Barnard, T. et al. Nitrogen cycling in CMIP6 land surface models: Progress and limitations. *Biogeosciences* **17**, 5129–5148 (2020).
49. Raich, J. W. & Schlesinger, W. H. The global carbon dioxide flux in soil respiration and its relationship to vegetation and climate. *Tellus B Chem. Phys. Meteorol.* **44**, 81–99 (1992).
50. Lawrence, D. M. et al. The community land model version 5: description of new features, benchmarking, and impact of forcing uncertainty. *J. Adv. Model. Earth Syst.* **11**, 4245–4287 (2019).
51. Koven, C. D., Lawrence, D. M. & Riley, W. J. Permafrost carbon–climate feedback is sensitive to deep soil carbon decomposability but not deep soil nitrogen dynamics. *Proc. Natl. Acad. Sci. USA* **112**, 3752–3757 (2015).
52. Oleson, K. et al. *Technical Description of Version 4.5 of the Community Land Model (CLM)* Technical Note NCAR/TN-503+STR (NCAR, 2013).
53. Schuur, E. A. G. et al. Climate change and the permafrost carbon feedback. *Nature* **520**, 171–179 (2015).
54. Van Huissteden, J. *Thawing Permafrost: Permafrost Carbon in a Warming Arctic* (Springer, Cham, 2020).
55. Turetsky, M. R. et al. Carbon release through abrupt permafrost thaw. *Nat. Geosci.* **13**, 138–143 (2020).
56. Burke, E. J., Zhang, Y. & Krinner, G. Evaluating permafrost physics in the Coupled Model Intercomparison Project 6 (CMIP6) models and their sensitivity to climate change. *Cryosphere* **14**, 3155–3174 (2020).
57. Slater, A. G. & Lawrence, D. M. Diagnosing present and future permafrost from climate models. *J. Clim.* **26**, 5608–5623 (2013).
58. Obu, J. et al. Northern Hemisphere permafrost map based on TTOP modelling for 2000–2016 at 1 km² scale. *Earth-Sci. Rev.* **193**, 299–316 (2019).

Acknowledgements

We thank Prof. Andrew H. MacDougall for insightful comments and discussions that greatly improved the paper. We acknowledge the World Climate Research Programme's Working Group on Coupled Modeling, which is responsible for CMIP, the climate modeling groups (listed in Supplementary Table 1) for producing and making their model output, and the Earth System Grid Federation for archiving the data and providing access. This research was supported by the R&D Program for Oceans and Polar Regions of the National Research Foundation (NRF) funded by the Ministry of Science and ICT (2020M1A5A110670) and supported by the National Research Foundation of Korea (NRF) grant funded by the Korean government (NRF-2022R1A3B1077622).

Author contributions

S.-W.P. compiled the data, conducted analyses, prepared the figures, and wrote the manuscript. J.-S.K. designed the research and wrote the majority of the manuscript content. All the authors discussed the study results and reviewed the manuscript.

Competing interests

The authors declare no competing interests.

Additional information

Supplementary information The online version contains supplementary material available at <https://doi.org/10.1038/s43247-022-00621-4>.

Correspondence and requests for materials should be addressed to Jong-Seong Kug.

Peer review information *Communications Earth & Environment* thanks the anonymous reviewers for their contribution to the peer review of this work. Primary Handling Editors: Clare Davis, Heike Langenberg.

Reprints and permission information is available at <http://www.nature.com/reprints>

Publisher's note Springer Nature remains neutral with regard to jurisdictional claims in published maps and institutional affiliations.



Open Access This article is licensed under a Creative Commons Attribution 4.0 International License, which permits use, sharing, adaptation, distribution and reproduction in any medium or format, as long as you give appropriate credit to the original author(s) and the source, provide a link to the Creative Commons license, and indicate if changes were made. The images or other third party material in this article are included in the article's Creative Commons license, unless indicated otherwise in a credit line to the material. If material is not included in the article's Creative Commons license and your intended use is not permitted by statutory regulation or exceeds the permitted use, you will need to obtain permission directly from the copyright holder. To view a copy of this license, visit <http://creativecommons.org/licenses/by/4.0/>.

© The Author(s) 2022